

# Experimental Characterization of a High Reynolds Number Turbulent Boundary Layer subjected to an Adverse Pressure Gradient

S. SRINATH<sup>a,b</sup>, C. CUVIER<sup>a,c</sup>, J.-M. FOUCAUT<sup>a,b</sup>, J.-P. LAVAL<sup>a,c</sup>,  
M. STANISLAS<sup>b</sup>, C. J. KAHLER<sup>d</sup>, R. HAIN<sup>d</sup>, S. SCHARNOWSKI<sup>d</sup>, A.  
SCHRÖDER<sup>d</sup>, R. GEISLER<sup>e</sup>, J. AGOCS<sup>e</sup>, A. RÖSE<sup>e</sup>, C. WILLERT<sup>f</sup>, J.  
KLINNER<sup>f</sup>, J. SORIA<sup>g</sup>, O. AMILI<sup>g</sup>, C. ATKINSON<sup>g</sup>

a. Univ. Lille, FRE 3723 -LML- Laboratoire de Mécanique de Lille, F-59000 Lille, France

b. Centrale Lille, F-59000 Lille, France

jean-marc.foucaut@centralelille.fr

c. CNRS, FRE 3723, F-59650 Villeneuve d'Ascq, France

d. Bundeswehr University Munich, Germany

e. DLR, Göttingen, Germany

f. DLR Köln, Germany

g. Monash University, Australia

## Résumé :

*Une couche limite turbulente se développe sur un profil a été étudiée expérimentalement dans le cadre du projet Européen EUHIT. Plusieurs expériences de PIV ont été réalisées dont une qui couvre toute l'épaisseur de la couche limite en gradient de pression adverse sur une longueur de plus de  $10\delta$  avec une bonne résolution spatiale. Les statistiques montrent le développement d'un second pic de Reynolds Stress caractéristique de ce type d'écoulement avec gradient de pression défavorable probablement associé à un renforcement des structures à grandes échelles.*

## Abstract :

*A turbulent boundary layer over a given geometry was studied experimentally in the framework of a EUHIT project. The geometry consists of a specifically designed ramp model, which is approximately 7 m long. The model used is the LML-AVERT ramp ([3]) on which the final flap was replaced by a 3.5m long flat plate (see figure 1). Several PIV experiments were conducted including one covering the full boundary layer thickness  $\delta$  over a length of more than  $10\delta$  with a good spatial resolution. The statistics show the development of a second peak characteristic of this type of flow with adverse pressure gradient and probably associated to the enhancement of very large scale motions.*

**Mots clefs :** Turbulent Boundary Layer, Particle Image Velocimetry, Adverse pressure gradient

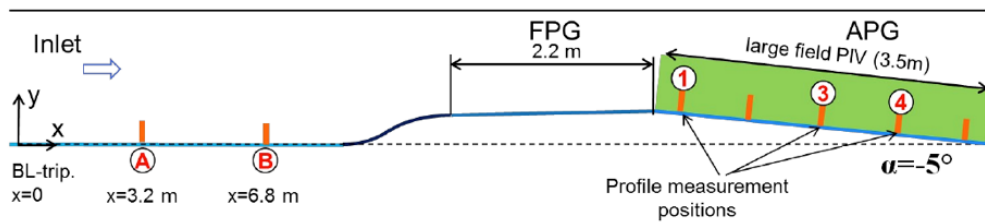


FIGURE 1: Sketch of the EUHIT experiments conducted in the LML wind tunnel.

## 1 Introduction

The observation of large-scale coherent structures in turbulent boundary layers has sparked great experimental and numerical interest. While most studies have focussed on channel flows and zero pressure gradient (ZPG) boundary layer flows, our understanding of wall turbulence under the influence of a streamwise pressure gradient is still quite limited due to the lack of sufficiently high Reynolds number data and large facilities to reach an equilibrium state [2], where theoretical scaling laws can be relevant. The length of these structures ( $7 - 14\delta$ ) [5] requires a large field of view and a high spatial resolution to measure all relevant spatial scales.

To resolve and characterize the structures in an adverse pressure gradient (APG) boundary layer, a set-up in the LML boundary layer wind tunnel was built using 16 sCMOS cameras (a consortium involving 4 teams under the framework of EuHIT) in order to perform large scale turbulent boundary layer measurements with appropriate spatial resolution [4]. The length of the 2D2C PIV measurement domain was 3.5m long and 0.25m high to ensure the possibility of capturing very large-scale structures with lengths more than  $10\delta$ . A total of 30000 images were recorded for two free-stream velocities of 5m/s and 9 m/s (corresponding to  $Re_\theta \approx 10600$  and  $Re_\theta \approx 17700$  respectively at station 4 of figure 1). The topology and dynamics of the large-scale turbulent structures under an APG will be presented. As a similar experiment with a large field of view (1.16m long and 0.3m high) was conducted earlier on a ZPG turbulent boundary layer at LML, the influence of an APG on these structures will be shown.

## 2 Experimental setup

The experiment was conducted as part of an EuHIT campaign in the LML boundary layer wind tunnel. The test section of  $1m \times 2m$  and  $20.6m$  long is fully transparent. This provides easy access to optical measurements and allows for excellent model viewing. The boundary layer is tripped at the wind tunnel entrance on both the top and bottom walls to fix the boundary layer transition. In the present studies, the wind tunnel was used in a closed loop configuration.

A sketch of the model geometry is shown in figure 1 where the flow is from left to right. The leading edge of the ramp was placed at 9.4m from the beginning of the test section. The platform consisted of a 1.33m long converging part, having a contraction ratio of 0.75. It was followed by a 2.2 m flat plate inclined at  $+1.5^\circ$  to the horizontal that generated a small favourable pressure gradient and a second plate of length 3.5 m inclined at  $-5^\circ$  to the horizontal where an APG region developed. The ramp was equipped with 51 pressure taps. 27 pressure taps for the streamwise pressure distribution and 24 for four transverse pressure distribution stations. Two stations are located each on the  $1.5^\circ$  plate and on the  $-5^\circ$  plate.

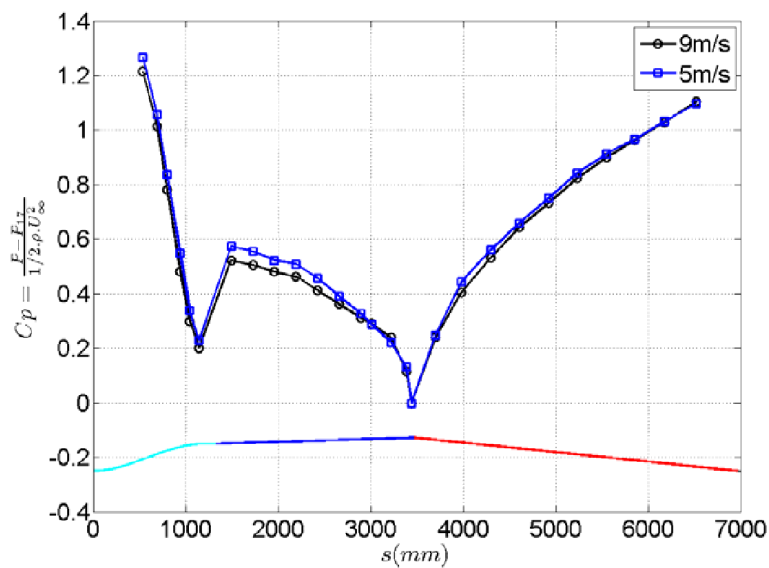


FIGURE 2: Distribution of the streamwise pressure coefficient along the ramp

### 3 Results

#### 3.1 Pressure distribution

The pressure distribution on the model was measured for two free-stream velocities ( $U_\infty = 5$  m/s and 9 m/s, both measured at the entrance of the wind tunnel). The pressure coefficient is defined as  $C_p = \frac{P - P_{17}}{\frac{1}{2}\rho U_\infty^2}$  where  $P_{17}$  being the reference pressure,  $\rho$  the density of air and  $U_\infty$  the free stream velocity upstream of the ramp located 10 cm downstream of the test section entrance. The pressure coefficient along the model for the two free stream velocities is shown in figure 2. The flow accelerates in the converging part  $0 \leq s \leq 1360$  mm of the ramp causing a decrease in the pressure coefficient until the suction peak at  $s=1146$  mm corresponding to pressure tap '6'. This suction peak then induces a locally strong adverse pressure gradient. Behind this suction peak, a region of pressure recovery occurs after which the flow begins to accelerate again due to the favourable pressure gradient caused by the 2.14 m long flat plate inclined at  $1.5^\circ$  to the wind tunnel floor. A second suction peak is observed at the articulation of the  $-5^\circ$  plate at  $s=3500$  mm close to the reference pressure tap 17. The 3.5 m long plate inclined at  $-5^\circ$  to the wind tunnel floor then causes a region of relatively constant adverse pressure gradient with a pressure gradient coefficient of about  $0.21m^{-1}$ . The pressure distribution on the top wall of the wind tunnel was also measured (see [4] for more detail)

#### 3.2 PIV results

An experimental setup consisting of 16 sCMOS cameras was built in order to study the boundary layer development in the region of an APG with a high spatial resolution while at the same time ensure the possibility of capturing the very large-scale turbulent structures. The field of view of each camera was 230 mm along the wall and about 270 mm in the wall normal direction. The light sheet was introduced to the tunnel using a mirror placed at  $45^\circ$  downstream to the ramp model that directed the laser sheet vertically upwards. The second mirror was located inside the test section, 87 cm downstream of the end of the ramp. This mirror directed the laser sheet along the 3.5m long APG section.

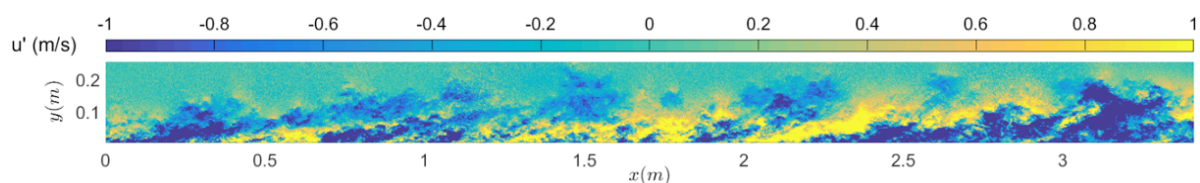
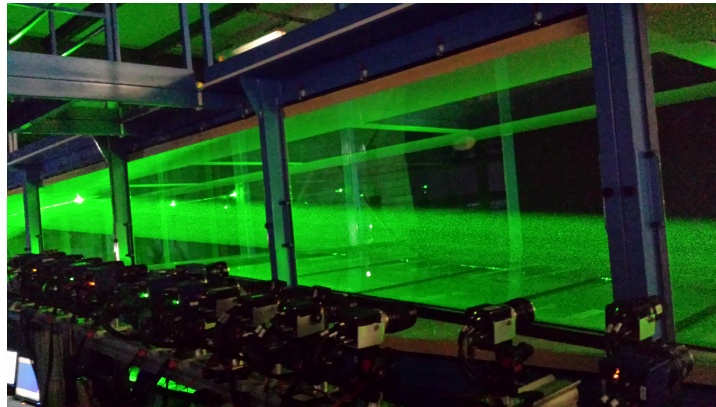


FIGURE 3: Setup of the 2D2C PIV with a 3.5m field of view (top) in the APG region ; sample of stream-wise velocity fluctuation (bottom).

A total of 30 000 samples were recorded at a frequency of 4 Hz for two free stream velocities of 5 and 9 m/s. The modified version of MatPIV toolbox by LML, under Matlab was used to process the acquired images. The mean background images were first mapped using a basic pinhole model and the reflection (i.e wall position was manually fitted with a line). A mesh was then built above this line in the mapped images (spacing of about 1.07 mm by 1.07 mm corresponding to 10 pixels by 10 pixels) and projected on each camera with the pinhole models. The analysis was then done with these projected grids. Four passes were used (24x24 pixels for the final one) with a mean overlap of 65%. The final grid have 3250 points along the wall and 238 points in the wall-normal direction corresponding to a region 3.41 m long and 0.25 m high with a grid spacing of 1mm. The 30000 samples lead to a convergence uncertainty of less than  $\pm 0.4\%$  on the mean streamwise velocity and on the mean wall normal velocity components and was estimated to be less than 2% for  $\overline{u'^2}$  and  $\overline{v'^2}$ .

Time Resolved High Magnification PIV (TRHM PIV) measurements were also conducted at three stations in the APG region ( $s = 3.983, 5.233$  and  $5.858$  m). Figures 4 show the mean streamwise velocity, streamwise and wall-normal turbulence intensities and the Reynolds shear stress profiles at these three stations. The profiles very close to the wall (shown in black) were obtained from TRHM PIV [6] while the profiles in the outer region (shown in blue) were obtained from the large field PIV. As seen in the figures 4, there is a good agreement between both methods. It is interesting to note that a logarithmic region exists on all the streamwise mean velocity profiles but with a limited extent in the wall normal direction ( $y^+$ ). Also, the high magnification measurements allow to resolve the near wall peak of the streamwise turbulent fluctuations which is at its usual location ( $y^+ \sim 15$ ). The presence of this peak is an indication of the existence of near wall streaks all along the APG region. Scaled with viscous units, the inner peak is nearly constant while the outer peak grows outward to reach a level comparable to the near wall peak at the last station. On the two other stress components, only the outer peak is clearly

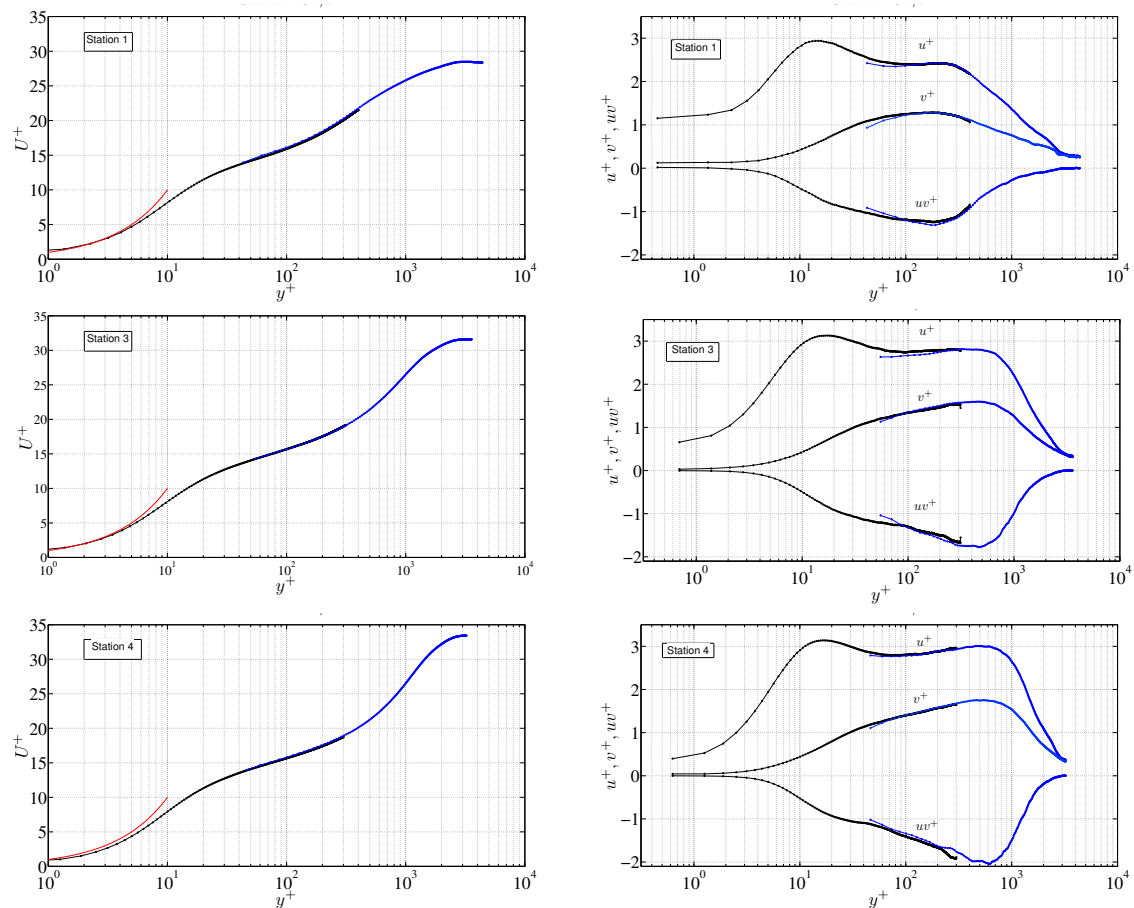


FIGURE 4: Mean velocity profiles (left) and streamwise fluctuating velocity profile (right) from the large 2D2C PIV field (blue lines) with the free-stream velocities ( $U_\infty = 5$  m/s) at three stations on the ramp (see figure 1). The near wall profile is obtained from a Time-resolved high magnification PIV conducted in the same project (see [4] for more details)

visible and it is also moves outward as we travel downstream.

## 4 Conclusion

A detailed experiment was conducted in order to characterize the turbulence in a mild adverse pressure gradient region produced by a model which reproduce the global behavior of an extrado of the wing. The flow field was characterized using multiple PIV setups with a very good spatial resolutions. A complete database gathering all the data from these experiments was made available [1]. This database can be used to investigate the scaling behavior of turbulent boundary layer with pressure gradient. As the inlet conditions are also provided, this experiment is well suited for detailed validation of turbulence models which are known to give poor results for such flows with adverse pressure gradient.

## 5 Acknowledgement

This work was carried out within the framework of the CNRS Research Federation on Ground Transports and Mobility, in articulation with the ELSAT2020 project supported by the European Community, the EUHIT project in the frame of its Transnational Access activity, the French Ministry of Higher Education and Research, the Hauts de France Regional Council. The authors gratefully acknowledge the support of these institutions.

## Références

- [1] Adverse pressure gradient turbulent boundary layer : Streamwise plane. [https://turbase.cineca.it/init/routes/#/logging/view\\_dataset/67/tabmeta](https://turbase.cineca.it/init/routes/#/logging/view_dataset/67/tabmeta). Accessed : 2015-08-04.
- [2] L. Castillo and W.K. George. Similarity analysis for turbulent boundary layer with pressure gradient : outer flow. *AIAA journal*, 39(1) :41–47, 2001.
- [3] C. Cuvier, J.-M. Foucaut, C. Braud, and M. Stanislas. Characterisation of a high reynolds number boundary layer subject to pressure gradient and separation. *Journal of Turbulence*, 15(8) :473–515, 2014.
- [4] C. Cuvier, S. Srinath, M. Stanislas, J.-M. Foucaut, J.-P. Laval, C.J. Kähler, R. Hain, S. Scharnowski, A. Schröder, R. Geisler, et al. Extensive characterization of a high reynolds number decelerating boundary layer using advanced optical metrology. *arXiv preprint arXiv :1702.02834*, 2017.
- [5] N. Hutchins and I. Marusic. Evidence of very long meandering features in the logarithmic region of turbulent boundary layers. *Journal of Fluid Mechanics*, 579 :1–28, 2007.
- [6] C.E Willert. High-speed particle image velocimetry for the efficient measurement of turbulence statistics. *Experiments in Fluids*, 56(1) :17, 2015.